

Fermiophobic light Higgs boson in the type-I two-Higgs-doublet model

Jinheung Kim,^{1,*} Soojin Lee,^{1,†} Prasenjit Sanyal,^{2,‡} and Jeonghyeon Song^{1,§}

¹*Department of Physics, Konkuk University, Seoul 05029, Republic of Korea*

²*Asia Pacific Center for Theoretical Physics, Pohang 37673, Republic of Korea*

Abstract

The null results in the new physics searches at the LHC do not exclude an intermediate-mass new particle if it is fermiophobic. Type-I in the two-Higgs-doublet model accommodates a fermiophobic light Higgs boson h_f if $\alpha = \pi/2$. The heavier CP -even Higgs boson explains the observed Higgs boson at a mass of 125 GeV. We first obtain the still-valid parameter space satisfying the theoretical requirements, flavor-changing neutral currents in B physics, the cutoff scale above 1 TeV, Higgs precision data, and the direct collider search bounds at high energy colliders. We also study the high energy scale behavior via the analysis of the renormalization group equations. An important result is that the fermiophobic type-I can maintain the stability of the scalar potential all the way up to the Planck scale if m_{h_f} is larger than half the observed Higgs boson mass. Since the parameter space is severely curtailed, especially for the high cutoff scale, the signal rates in the multi-photon states of new Higgs bosons at the LHC are well predicted. We suggest the processes of $4\gamma + VV'$ ($V^{(\prime)} = Z, W^\pm$) as the golden discovery channels for the model since they enjoy an almost background-free environment and substantial selection efficiencies for four photons.

Keywords: Higgs Physics, Beyond the Standard Model

arXiv:2207.05104v1 [hep-ph] 11 Jul 2022

*Electronic address: jinheung.kim1216@gmail.com

†Electronic address: soojinlee957@gmail.com

‡Electronic address: prasenjit.sanyal@apctp.org

§Electronic address: jhsong@konkuk.ac.kr

Contents

I. Introduction	2
II. Fermiophobic h in type-I 2HDM	3
III. Scanning strategies and model validity	5
IV. LHC phenomenology	9
V. Conclusions	13
Acknowledgments	14
References	14

I. INTRODUCTION

The standard model (SM) of particle physics has achieved unprecedented success in explaining almost all the experimental data at high energy colliders. Nevertheless, we firmly believe that there is new physics beyond the SM (BSM) because the SM does not have the answers for the naturalness problem, the fermion mass hierarchy, the origin of CP violation in the quark sector, the baryogenesis, the non-zero neutrino masses, and the identity of dark matter. In the hope that a new physics signal is just around the corner, the ATLAS and CMS collaborations have tried hard to find a new particle, but not succeeded so far.

The absence of a new signal in the current data set at the LHC is usually attributed to very heavy or very light masses of new particles. But there exists an intriguing alternative, a fermiophobic new particle. If a new particle does not couple to the SM fermions, its production via quark-antiquark annihilation is highly suppressed. If the new particle is a color singlet as suggested in many BSM models, the gluon fusion production through quark loops is also forbidden. The infeasibility of the direct production of a fermiophobic particle naturally explains the absence of new signals at the LHC. In this regard, there have been extensive theoretical studies on the fermiophobic BSM particle such as a Higgs boson [1–16], gauge boson [17–24], and unparticle [25]. In the experimental side, a fermiophobic Higgs boson has been searched for in the diphoton mode at the LEP-2 [26, 27], Tevatron [28–31], and LHC [32–35].

Nevertheless criticism can follow that a BSM model with a fermiophobic particle is introduced as an ad hoc just to evade the disappointing situation of no new signals at the electroweak scale. One way to value the BSM model is to investigate the high energy scale behavior through the analysis of the renormalization group equations (RGE). If the model remains theoretically valid up to very high energy scale like the Planck scale, it will become a better candidate for the UV theory. The RGE analysis requires one specific BSM model. Type I in the two-Higgs-doublet model (2HDM) is one of the most attractive BSM models to offer a fermiophobic Higgs

boson: all the Yukawa couplings of a new CP -even neutral Higgs boson φ^0 are the same in type I so that a single condition can guarantee the fermiophobic nature of φ^0 . The observation of the SM-like Higgs boson at the LHC [36–38] can be explained in two ways, the normal scenario where the lighter CP -even Higgs boson is observed and the inverted scenario where the heavier CP -even Higgs boson is observed [39–42]. Considering the experimental searches for a light fermiophobic Higgs boson via diphoton mode, we focus on the inverted scenario of type I in this letter.

The study of the high energy scale behavior of the fermiophobic type-I requires the basic work of extracting all the viable parameter points that satisfy the theoretical and experimental constraints, via random scanning of the entire parameter space. In the literature, the Higgs precision data and the direct search bounds are usually checked by the public codes of HIGGSIGNALS [43] and HIGGSBOUNDS [44], respectively. However, even the most recent version HIGGSBOUNDS-v5.10.2 misses three important processes for a light fermiophobic Higgs boson, multi-photon signals measured by the DELPHI [27], CDF [45], and CMS collaborations [46]. We need to include the three processes in the random scanning. Based on the finally allowed parameter points, we will perform for the first time the RGE analysis to obtain the cutoff scale of every viable parameter point. In addition, we will study the decays and productions of the BSM Higgs bosons to suggest $4\gamma + VV'$ as the golden discovery channel at the HL-LHC, which complements the studies of $4\gamma + V$ in the literature [6, 7, 15, 47, 48]. In addition to presenting the cross section times branching ratio as well as the selection efficiencies at the detector level, we will also present the correlation between the cutoff scale and the signal rates. These are our new contributions.

The paper is organized in the following way. In Sec. II, we give a brief review of the fermiophobic type-I in the 2HDM. In Sec. III, we do the parameter scanning by imposing the theoretical and experimental constraints, including the RGE analysis. Section IV deals with the LHC phenomenology of the BSM Higgs bosons. Finally we conclude in Sec. V.

II. FERMIOPHOBIC h IN TYPE-I 2HDM

In the 2HDM, there exist two $SU(2)_L$ complex scalar doublet fields with hypercharge $Y = +1$ [49]:

$$\Phi_i = \begin{pmatrix} w_i^+ \\ \frac{v_i + \rho_i + i\eta_i}{\sqrt{2}} \end{pmatrix}, \quad (i = 1, 2) \quad (1)$$

where v_1 and v_2 are the vacuum expectation values of Φ_1 and Φ_2 respectively. The electroweak symmetry is spontaneously broken by the nonzero vacuum expectation value of $v = \sqrt{v_1^2 + v_2^2} = 246$ GeV. The ratio of v_2 to v_1 is defined by $\tan\beta = v_2/v_1$ ($\beta \in [0, \pi/2]$). For notational simplicity, we take $s_x = \sin x$, $c_x = \cos x$, and $t_x = \tan x$ in what follows. A discrete Z_2 symmetry is introduced to prevent the tree level flavor-changing neutral currents (FCNC) [50,

[51], under which $\Phi_1 \rightarrow \Phi_1$ and $\Phi_2 \rightarrow -\Phi_2$. Then the scalar potential with softly broken Z_2 symmetry and CP -invariance is

$$\begin{aligned}
V_\Phi = & m_{11}^2 \Phi_1^\dagger \Phi_1 + m_{22}^2 \Phi_2^\dagger \Phi_2 - m_{12}^2 (\Phi_1^\dagger \Phi_2 + \text{H.c.}) \\
& + \frac{1}{2} \lambda_1 (\Phi_1^\dagger \Phi_1)^2 + \frac{1}{2} \lambda_2 (\Phi_2^\dagger \Phi_2)^2 + \lambda_3 (\Phi_1^\dagger \Phi_1) (\Phi_2^\dagger \Phi_2) + \lambda_4 (\Phi_1^\dagger \Phi_2) (\Phi_2^\dagger \Phi_1) \\
& + \frac{1}{2} \lambda_5 \left[(\Phi_1^\dagger \Phi_2)^2 + \text{H.c.} \right].
\end{aligned} \tag{2}$$

Five physical Higgs bosons exist, the light CP -even scalar h , the heavy CP -even scalar H , the CP -odd pseudoscalar A , and a pair of charged Higgs bosons H^\pm . The mass eigenstates are related with the weak eigenstates in Eq. (1) via two mixing angles of α and β , of which the relations are referred to Ref. [52]. The SM Higgs boson is a linear combination of h and H , given by

$$h_{\text{SM}} = s_{\beta-\alpha} h + c_{\beta-\alpha} H. \tag{3}$$

The observed SM-like Higgs boson at a mass of 125 GeV can be either h or H . In this work, we concentrate on the inverted scenario where $M_H = 125$ GeV. Then the Higgs coupling modifiers to V ($V = W^\pm, Z$) are

$$\kappa_V^H = c_{\beta-\alpha}, \quad \xi_V^h = s_{\beta-\alpha}. \tag{4}$$

Note that the SM-like Higgs boson demands $|s_{\beta-\alpha}| \ll 1$. For the sign of $c_{\beta-\alpha}$, we adopt the scheme with $c_{\beta-\alpha} > 0$ as in the public codes such as 2HDMC [53], HIGGSIGNALS [43], and HIGGSBOUNDS [44].

We parameterize the Yukawa interactions of the SM fermions as

$$\begin{aligned}
\mathcal{L}^{\text{Yuk}} = & - \sum_f \left(\frac{m_f}{v} \xi_f^h \bar{f} f h + \frac{m_f}{v} \kappa_f^H \bar{f} f H - i \frac{m_f}{v} \xi_f^A \bar{f} \gamma_5 f A \right) \\
& - \left\{ \frac{\sqrt{2}}{v} \bar{t} (m_t \xi_t^A P_- + m_b \xi_b^A P_+) b H^+ + \frac{\sqrt{2} m_\tau}{v} \xi_\tau^A \bar{\nu}_\tau P_+ \tau H^+ + \text{H.c.} \right\},
\end{aligned} \tag{5}$$

where $f = t, b, \tau$ and $P_\pm = (1 \pm \gamma^5)/2$. In type-I, the normalized Yukawa couplings are

$$\xi_f^h = \frac{c_\alpha}{s_\beta}, \quad \kappa_f^H = \frac{s_\alpha}{s_\beta}, \quad \xi_t^A = -\xi_b^A = -\xi_\tau^A = \frac{1}{t_\beta}. \tag{6}$$

If $\alpha = \pi/2$, $\xi_f^h = 0$ so that h becomes fermiophobic. We assume that the fermiophobic condition is preserved at loop level by a suitable renormalization condition [4, 5]. To emphasize the fermiophobic nature, we take the notation of h_f for the light CP -even Higgs boson with vanishing Yukawa couplings to the SM fermions. Our model is summarized as

$$M_H = 125 \text{ GeV}, \quad \alpha = \frac{\pi}{2}. \tag{7}$$

Since $t_\beta = -c_{\beta-\alpha}/s_{\beta-\alpha}$ if $\alpha = \pi/2$, the condition of $|s_{\beta-\alpha}| \ll 1$ corresponds to $t_\beta \gg 1$.

III. SCANNING STRATEGIES AND MODEL VALIDITY

We scan the parameter space by imposing all the theoretical and experimental constraints. To efficiently satisfy the oblique parameters of S , T , and U , we make the assumption of $M_A = M_{H^\pm} \equiv M_{A/H^\pm}$. Then there are four model parameters, m_{h_τ} , M_{A/H^\pm} , t_β , and m_{12}^2 . For the fixed m_{h_τ} of

$$m_{h_\tau} = 20, 30, 40, 60, 96 \text{ GeV}, \quad (8)$$

we randomly generate the other parameters over the ranges of

$$\begin{aligned} M_{A/H^\pm} &\in [80, 900] \text{ GeV}, \\ t_\beta &\in [1, 100], \quad m_{12}^2 \in [0, 15000] \text{ GeV}^2. \end{aligned} \quad (9)$$

Now we cumulatively impose the following constraints:

Step-A. Theoretical constraints with low energy data:

- (1) We require the Higgs potential being bounded from below [54], the unitarity of scalar-scalar scatterings [49, 55], the perturbativity of Higgs quartic couplings [40], and the stability of the CP -conserving vacuum [56–58]. The public code 2HDMC [53] is used.
- (2) We demand the Peskin-Takeuchi electroweak oblique parameters S , T , and U [59] to satisfy the current best-fit results [60] at 95% C.L.:

$$\begin{aligned} S &= -0.01 \pm 0.10, \quad T = 0.03 \pm 0.12, \quad U = 0.02 \pm 0.11, \\ \rho_{ST} &= 0.92, \quad \rho_{SU} = -0.80, \quad \rho_{TU} = -0.93, \end{aligned} \quad (10)$$

where ρ_{ij} is the correlation matrix. We use the 2HDM calculations of S , T , and U in Refs. [60–62].

- (3) We require that the most recent constraints from flavor physics be satisfied at 95% C.L. [63, 64]. An important constraint is from $b \rightarrow s\gamma$, which excludes the region with small t_β and the light charged Higgs boson: for example, $\tan\beta > 2.6$ for $M_{H^+} = 140 \text{ GeV}$ [63].
- (4) We demand that the model be valid at least up to 1 TeV, i.e., the cutoff scale Λ_c be larger than 1 TeV. Λ_c is obtained through the following procedures:
 - For each parameter point, we perform the RGE running at one loop level, starting from the top quark pole mass scale, $m_t^{\text{pole}} = 173.4 \text{ GeV}$. The boundary conditions at m_t^{pole} are referred to Ref. [65]. We use the open code 2HDME [66].
 - At the next high energy scale, we check three conditions—unitarity, perturbativity, and vacuum stability. If any condition is broken, we stop the running and record the energy scale as the cutoff scale Λ_c .

	Survival probabilities				
m_{h_f} [GeV]	20	30	40	60	96
Step-B(2)	1.10%	0.27%	0.13 %	0.026 %	25.7%
Step-B(3)	0.207%	0.048%	0.011%	0.000%	25.7%

TABLE I: Survival probabilities at Step-B(2) and Step-B(3) for $m_{h_f} = 20, 30, 40, 60, 96$ GeV. The reference is the parameter point that pass Step-A.

Step-B. High energy collider data:

- (1) We check whether each parameter point satisfies the Higgs precision data. We use the public code HIGGSIGNALS-v2.6.2 [43], which gives the χ^2 value for 111 Higgs observables [67–74]. We demand that the p -value should be larger than 0.05.
- (2) The parameter point should not conflict with the null results of the direct searches at the LEP, Tevatron, and LHC. Using the open code HIGGSBOUNDS-v5.10.2 [44], we exclude a parameter point if the predicted cross section is larger than 95% C.L. upper bound on the observed cross section.
- (3) Three important processes for a light fermiophobic Higgs boson are missing in HIGGSBOUNDS, the DELPHI measurement of $\gamma\gamma Z/\gamma\gamma b\bar{b}$ states [27], the CDF measurement of $4\gamma W^\pm$ [45], and the CMS search for 4γ [46]. We include the constraints from these processes.

For each m_{h_f} in Eq. (8), we first obtained 1.2×10^6 parameter points that pass Step-A, over which we imposed the constraints at Step-B. The Higgs precision data and the direct search bounds severely constrain the model. The three processes in Step-B(3) additionally remove the parameter points. To quantify the curtailment of the parameter space, we separately show the survival probabilities at Step-B(2) and Step-B(3) in Table I, with respect to the parameter points after Step-A. We first focus on Step-B(2). For $m_{h_f} \lesssim m_{125}/2$, the fermiophobic type-I barely survives with the probability below $\mathcal{O}(1)\%$. The killer processes are the ATLAS measurement of $h_{\text{SM}} \rightarrow h_f h_f \rightarrow 4\gamma$ [75] and the LEP measurement of $e^+e^- \rightarrow h_f Z \rightarrow \gamma\gamma + Z$ [76]. For $m_{h_f} = 96$ GeV, on the other hand, a large portion of the parameter space remains valid with the survival probability of about 25% at Step-B(2). The smoking-gun processes are the ATLAS measurements of $t \rightarrow H^\pm b \rightarrow \tau\nu + b$ [77] and $pp \rightarrow h_f/W h_f/Z h_f/tth_f \rightarrow \gamma\gamma + X$ [78].

Let us discuss the three processes at Step-B(3). The first is the DELPHI search for a fermiophobic Higgs boson in the multi-photon states [27], which consists of $e^+e^- \rightarrow h_f(\rightarrow \gamma\gamma)Z$ and $e^+e^- \rightarrow h_f(\rightarrow \gamma\gamma)A(\rightarrow b\bar{b}/h_f Z)$. For $m_{h_f} = 30$ GeV, the DELPHI results exclude $M_A \leq 148$ GeV, which reduces the survival probability at Step-B(2) by about 80%. For $m_{h_f} = 96$ GeV, however, the DELPHI results do not affect because of the heavy mass. The second is the CDF measurement of $p\bar{p} \rightarrow H^\pm(\rightarrow W^\pm h_f)h_f \rightarrow 4\gamma + X$ [45]. Based on the assumptions of $\mathcal{B}(h_f \rightarrow \gamma\gamma) = 1$ and $M_A = 350$ GeV, the CDF collaboration presented the excluded region of

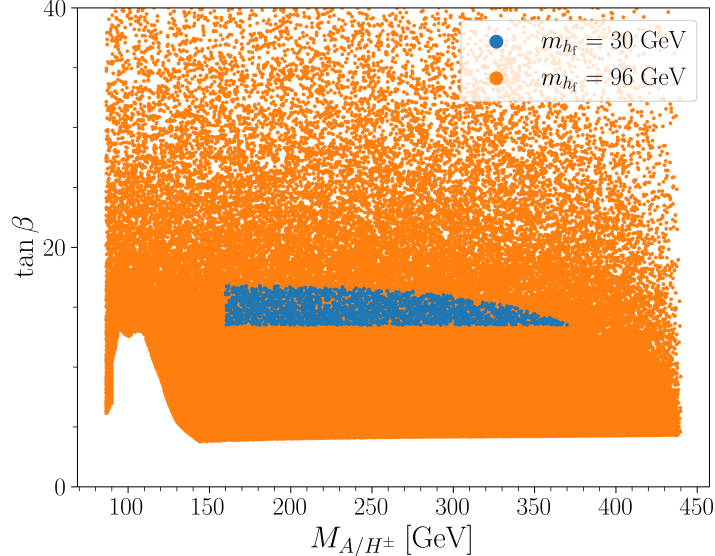


FIG. 1: $\tan\beta$ versus M_{A/H^\pm} for $m_{h_f} = 30$ GeV (blue points) and $m_{h_f} = 96$ GeV (orange points).

(M_{H^\pm}, m_{h_f}): for $m_{h_f} = 30$ GeV, $M_{H^\pm} \leq 160$ GeV is prohibited. But the case of $m_{h_f} = 96$ GeV is not affected by the CDF measurement since $\mathcal{B}(h_f \rightarrow \gamma\gamma) \lesssim 0.25$ as shall be shown below. The third is the CMS search for the exotic decay of the Higgs boson into four-photon final states in the mass range of $m_{h_f} \in [10, 60]$ GeV [46]: for $m_{h_f} = 30$ GeV, $\sigma \times \mathcal{B} \leq 0.9$ fb. An extraordinary case is for $m_{h_f} = 60$ GeV. Out of 1.2×10^6 points after Step-A, only about 300 points survive Step-B(2) and no parameter point remains after Step-B(3). The smoking-gun processes at Step-B(2) are the exotic Higgs decay of $h_{\text{SM}} \rightarrow h_f h_f \rightarrow 4\gamma$ and the LHC process of $gg \rightarrow A \rightarrow Z^{(*)}(\rightarrow \ell^+ \ell^-) h_{\text{SM}}(\rightarrow b\bar{b})$ [79], which permits $M_{H^\pm} \in [80, 120]$ GeV. Then the DELPHI and CDF results exclude the light M_{A/H^\pm} region.

We investigate the characteristics of the finally allowed parameter space. Figure 1 shows t_β versus M_{A/H^\pm} for $m_{h_f} = 30$ GeV (blue points) and $m_{h_f} = 96$ GeV (orange points). Both cases have the upper bounds on the masses of A and H^\pm : $M_{A/H^\pm} \lesssim 360$ GeV for $m_{h_f} = 30$ GeV and $M_{A/H^\pm} \lesssim 440$ GeV for $m_{h_f} = 96$ GeV. The lower bound on M_{A/H^\pm} also exists, $M_{A/H^\pm} \gtrsim 160$ GeV for $m_{h_f} = 30$ GeV and $M_{A/H^\pm} \gtrsim 90$ GeV for $m_{h_f} = 96$ GeV. The larger lower bound on M_{A/H^\pm} for $m_{h_f} = 30$ GeV is from the constraints at Step-B(3). In addition, we have substantially large t_β for $m_{h_f} = 30$ GeV, above about 13. For $m_{h_f} = 96$ GeV, however, t_β can be as small as about 3. The relation of $t_\beta = -c_{\beta-\alpha}/s_{\beta-\alpha}$ in the fermiophobic type-I translates t_β into $s_{\beta-\alpha}$. We have $|s_{\beta-\alpha}| \lesssim 0.08$ for $m_{h_f} = 30$ GeV and $|s_{\beta-\alpha}| \lesssim 0.27$ for $m_{h_f} = 96$ GeV. Considerable deviation from the Higgs alignment can occur when m_{h_f} is heavier than half the observed Higgs boson mass.

Although the fermiophobic type-I is shown to satisfy all the theoretical and experimental constraints, this validity is only at the electroweak scale. Then to what energy scale is this model valid? Focusing on two cases with $m_{h_f} = 30, 96$ GeV, we calculate the cutoff scale for each parameter point after Step-B(3). Figure 2 shows the distribution of Λ_c . The y -axis represents the ratio $N_{\text{cutoff}}/N_{\text{total}}$, where N_{cutoff} is the number of the parameter points with the

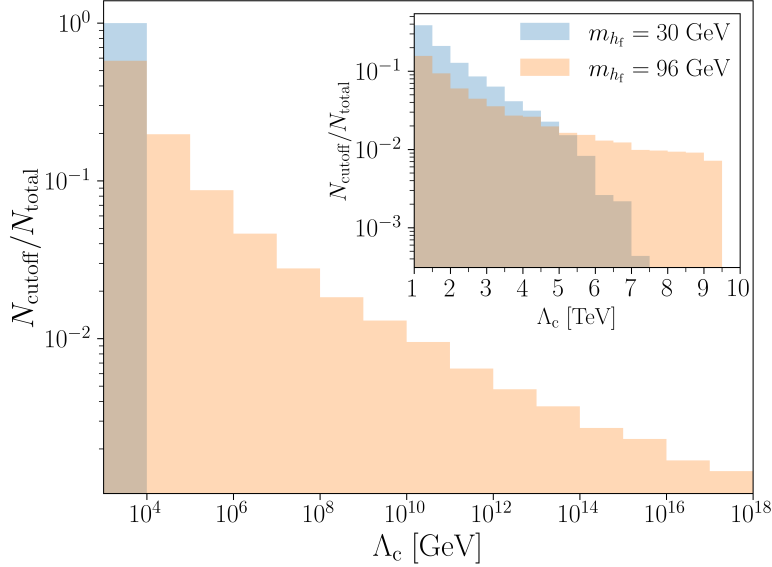


FIG. 2: Distributions of the cutoff scales of the finally allowed parameter points for $m_{h_f} = 30, 96$ GeV.

cutoff scale Λ_c and N_{total} is the total number of the finally allowed parameter points. It is clearly seen that the case of $m_{h_f} = 30$ GeV has quite low cutoff scales. A very light fermiophobic Higgs boson is not only difficult to satisfy the current data (see the small survival probabilities in Table I) but also unable to maintain stability above 10 TeV. It demands an extension at the energy scale not far from the LHC reach. If $m_{h_f} = 96$ GeV, however, the scalar potential can be stable all the way up to the Planck scale. The parameter ranges with $\Lambda_c > 10^{18}$ GeV are

$$\begin{aligned}
 m_{h_f} = 96 \text{ GeV with } \Lambda_c > 10^{18} \text{ GeV : } & M_{A/H^\pm} \in [94.9, 149.7] \text{ GeV}, \\
 & m_{12}^2 \in [97.8, 2071.7] \text{ GeV}^2, \\
 & s_{\beta-\alpha} \in [-0.22, -0.01], \quad t_\beta \in [4.34, 94.3],
 \end{aligned} \tag{11}$$

which prefer intermediate masses for A and H^\pm .

Finally, we make brief comments on the recent measurement of the W boson mass by the CDF collaboration, $m_W^{\text{CDF}} = 80.4335 \pm 0.0094$ GeV [80]. If we take m_W^{CDF} as a face value, it shows 7σ deviation from the SM prediction, which yields different oblique parameters as $S_{\text{CDF}} = 0.15 \pm 0.08$ and $T_{\text{CDF}} = 0.27 \pm 0.06$ with $U = 0$ [81]. Although the implications of the anomaly in the framework of the 2HDM have been extensively studied [42, 81–95], the fermiophobic type-I has not been considered in the literature. So we rescanned the parameter space with S_{CDF} and T_{CDF} . With the condition of $\Delta M_A (\equiv M_A - M_{H^\pm}) = 0$, no parameter point survives even Step-A(2). If the mass degeneracy is relaxed to $\Delta M_A = -20$ GeV, many parameter points pass Step-A(3), but no point satisfies the condition of $\Lambda_c > 1$ TeV at Step-A(4). If $\Delta M_A = -30$ GeV, a large portion of the parameter space passes the final step. In summary, the CDF W boson mass measurement demands a sizable (but not large) mass gap between A and H^\pm .

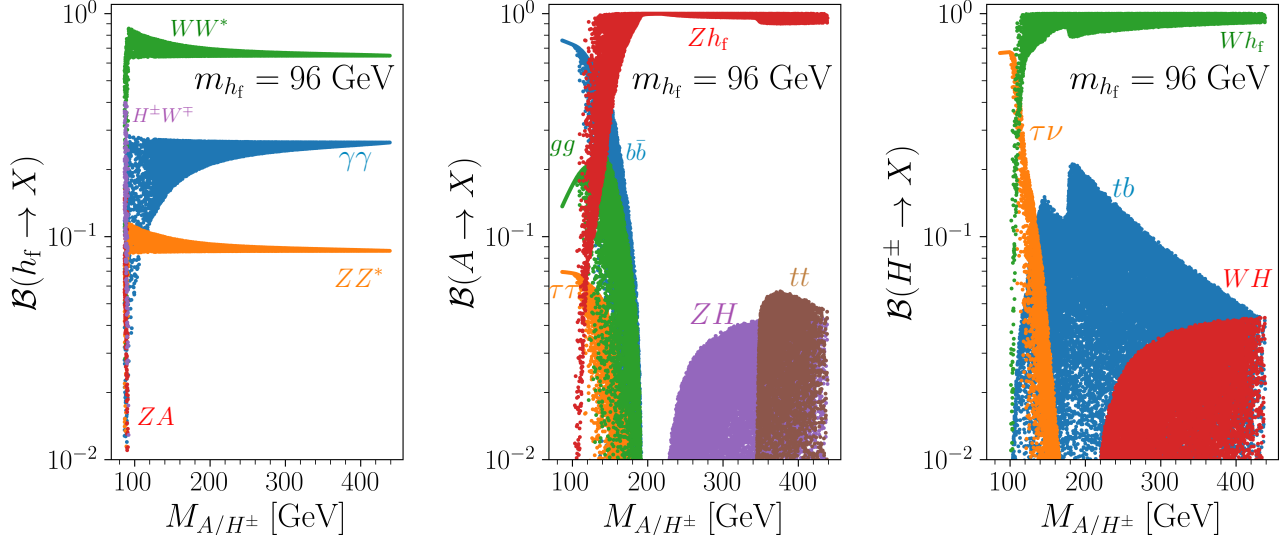


FIG. 3: Branching ratios of h_f (left panel), A (middle panel), and H^\pm (right panel) for $m_{h_f} = 96$ GeV.

IV. LHC PHENOMENOLOGY

Now that the finally allowed parameter space is significantly limited, the observation of the fermiophobic type-I at the LHC is more predictive than ever. We first discuss the decays of h_f , which are only into electroweak bosons: the loop-induced decay of $h_f \rightarrow gg$ also vanishes because it occurs through quarks. The off-shell decays of h_f into VV^* is feasible due to the deviation from the Higgs alignment, especially in the case of $m_{h_f} = 96$ GeV. The radiative decay of h_f into $\gamma\gamma$ gets the contribution from W^\pm and H^\pm in the loop. The coupling for the h_f - H^+ - H^- vertex is

$$\hat{\lambda}_{hH^+H^-} = \frac{1}{v^2} \left[(2M_{H^\pm}^2 - m_{h_f}^2)c_\beta + \frac{m_{h_f}^2 - M^2}{c_\beta} \right] \simeq \frac{t_\beta}{v^2} (m_{h_f}^2 - M^2), \quad (12)$$

where $M^2 = m_{12}^2/(s_\beta c_\beta)$ and $\hat{\lambda}_{hH^+H^-}$ is defined by $\mathcal{L}_{\text{tri}} \supset v \hat{\lambda}_{hH^+H^-} h_f H^+ H^-$. Since the finally allowed parameter points prefer large t_β and intermediate M_{H^\pm} , the decay mode of $h_f \rightarrow \gamma\gamma$ will be important.

The branching ratios of the BSM Higgs bosons crucially depend on the mass of h_f . Let us first consider the case of $m_{h_f} = 30$ GeV. Very light h_f exclusively decays into $\gamma\gamma$ with $\mathcal{B}(h_f \rightarrow \gamma\gamma) \simeq 100\%$. The other BSM Higgs bosons, A and H^\pm , also have a single dominant decay mode, $A \rightarrow Zh_f$ and $H^\pm \rightarrow W^\pm h_f$, which have almost 100% branching ratios. The main reason is the kinematic gain from the light m_{h_f} and the heavy enough M_{A/H^\pm} as shown in Fig. 1.

In the case of $m_{h_f} = 96$ GeV, the decay patterns of the BSM Higgs bosons are more diverse. Figure 3 shows the branching ratios of h_f (left panel), A (middle panel), and H^\pm (right panel) as a function of M_{A/H^\pm} , over the finally allowed parameter points. The leading decay mode of h_f is into WW^* with the branching ratio of about 70%. We ascribe it to the sizable deviation from the Higgs alignment and the tree-level decay. The diphoton mode is next-to-leading with

$\mathcal{B}(h_f \rightarrow \gamma\gamma) \lesssim 28\%$. The third dominant decay mode is $h_f \rightarrow ZZ^*$ with the branching ratio of about 10%. The pseudoscalar A has the most diverse decay modes among the BSM Higgs bosons. For $M_A \lesssim 120$ GeV, $A \rightarrow b\bar{b}$ is the leading decay mode, followed by $A \rightarrow gg$ and $A \rightarrow \tau^+\tau^-$. For $M_A \gtrsim 150$ GeV, the bosonic mode of $A \rightarrow Zh_f$ becomes dominant. Above the kinematic threshold, the decays of $A \rightarrow ZH$ and $A \rightarrow t\bar{t}$ can be substantial with a few percent branching ratios. The charged Higgs boson mainly decays into $W^\pm h_f$ [96] except for small mass window of $M_{H^\pm} \in [80, 110]$ GeV where $H^\pm \rightarrow \tau\nu$ is dominant. Above the kinematic threshold, the branching ratios of $H^\pm \rightarrow tb$ and $H^\pm \rightarrow W^\pm H$ can be of the order of 1%.

Brief comments on the possibility of h_f as a long-lived particle are in order here. If the total decay width of h_f is small enough to make h_f long-lived, we see a signal of a photon pair from the secondary vertex displaced from the primary vertex. If a particle has $\Gamma_{\text{tot}} = 10^{-11}$ GeV, for example, the decay length $d \simeq \beta\gamma \times 10^{-6}$ m where $\gamma = E/m$ and $\beta = v/c$. Since photons do not leave any track in the inner tracker, we have to deduce the secondary vertex from the photon tracks in the ECAL. In Ref. [97], it was shown that we need the decay length larger than 0.1 cm to probe the signal, which require $\Gamma_{\text{tot}} < 10^{-13}$ GeV even with $\gamma = 10$. We find that the minimum of $\Gamma_{\text{tot}}^{h_f}$ is 1.3×10^{-12} GeV for $m_{h_f} = 20$ GeV, 3.9×10^{-12} GeV for $m_{h_f} = 30$ GeV, and 1.9×10^{-9} GeV for $m_{h_f} = 96$ GeV. It is difficult to see the displaced diphoton signals of a long-lived h_f at the LHC in the fermiophobic type-I.

Considering the branching ratios of the BSM Higgs bosons, we study the following multi-photon states at the LHC:

$$4\gamma + Z : \quad pp \rightarrow A(\rightarrow Zh_f)h_f \rightarrow 4\gamma + Z, \quad (13)$$

$$pp \rightarrow H(\rightarrow h_f h_f)Z \rightarrow 4\gamma + Z,$$

$$4\gamma + W^\pm : \quad pp \rightarrow H^\pm(\rightarrow W^\pm h_f)h_f \rightarrow 4\gamma + W^\pm,$$

$$pp \rightarrow H(\rightarrow h_f h_f)W^\pm \rightarrow 4\gamma + W^\pm,$$

$$4\gamma + W^\pm Z : \quad pp \rightarrow H^\pm(\rightarrow W^\pm h_f)A(\rightarrow Zh_f) \rightarrow 4\gamma + W^\pm Z, \quad (14)$$

$$4\gamma + W^+W^- : \quad pp \rightarrow H^+(\rightarrow W^+ h_f)H^-(\rightarrow W^- h_f) \rightarrow 4\gamma + W^+W^-.$$

Note that the Higgs alignment favors the productions of $q\bar{q} \rightarrow Z^* \rightarrow HA$ and $q\bar{q}' \rightarrow W^* \rightarrow H^\pm A$.

In Fig. 4, we present as a function of M_{A/H^\pm} the production cross section times branching ratio for $4\gamma + Z$ (upper-left panel), $4\gamma + W^\pm$ (upper-right panel), $4\gamma + W^\pm Z$ (lower-left panel), and $4\gamma + W^+W^-$ (lower-right panel) over the finally allowed parameter points. We take two cases of $m_{h_f} = 30$ GeV and $m_{h_f} = 96$ GeV. The color code denotes the cutoff scale Λ_c . To calculate the parton-level production cross sections, we first use FEYNRULES [98] to obtain the Universal FeynRules Output (UFO) [99] for the fermiophobic type-I. Interfering the UFO file with MADGRAPH5-AMC@NLO [100], we compute the cross-sections of $pp \rightarrow Ah_f/HZ/H^\pm h_f/HW^\pm/H^\pm A/H^+H^-$ at 14 TeV LHC using NNPDF31_LO_AS_0118 parton distribution function set [101]. The two-body cross-sections are multiplied by relevant branching ratios of h_f , A , and H^\pm obtained from the 2HDMC [53].

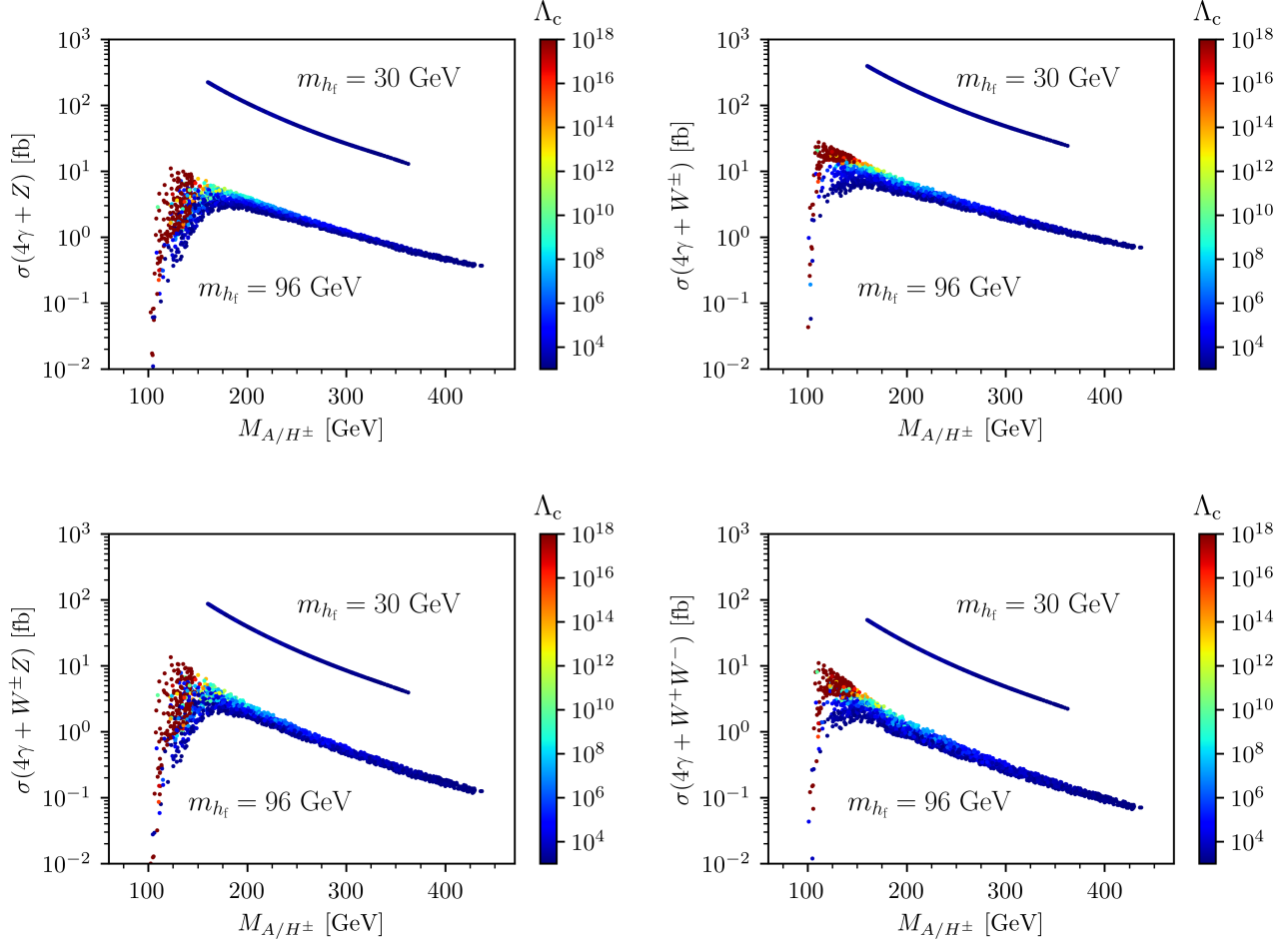


FIG. 4: Cross-section times branching ratio of multi-photon states as a function of M_{A/H^\pm} : $4\gamma + Z$ (upper-left panel), $4\gamma + W^\pm$ (upper-right panel), $4\gamma + W^\pm Z$ (lower-left panel), and $4\gamma + W^+W^-$ (lower-right panel) for $m_{h_f} = 30$ GeV and $m_{h_f} = 96$ GeV. The color code denotes the cutoff scale Λ_c .

The first noteworthy result in Fig. 4 is that the signal rate of $m_{h_f} = 30$ GeV is about ten times larger than that of $m_{h_f} = 96$ GeV for all the processes. This feature is attributed primarily to the kinematic advantage of very light m_{h_f} . Unexpected is the result that the signal rate of $4\gamma + VV'$ is almost compatible with that of $4\gamma + V$, even though $4\gamma + VV'$ has one more particle in the final state. It is because both $4\gamma + V$ and $4\gamma + VV'$ are basically $2 \rightarrow 2$ processes with large branching ratios: see Eqs. (13) and (14). Since $4\gamma + VV'$ has one more tagging particle, which is hard for the SM backgrounds to mimic, we suggest $4\gamma + VV'$ as the golden discovery channel for the light fermiophobic Higgs boson.

Now, let us discuss the correlation of the signal rate to cutoff scale. For the case of $m_{h_f} = 30$ GeV, which has a low cutoff scale below 7 TeV, there is no point in discussing the correlation. In the case of $m_{h_f} = 96$ GeV, however, the cutoff scale is widely distributed, from 1 TeV to the Planck scale. So, the correlation has a profound implication on the LHC phenomenology. The color code of Λ_c in Fig. 4 clearly shows that the maximum signal rate for all the multi-photon final states happens when the model has $\Lambda_c \sim 10^{18}$ GeV.

selection efficiency $\epsilon_d = \sigma(\text{cuts})/\sigma(\text{no cuts})$					
		$4\gamma + WW$		$4\gamma + WZ$	
	$(m_{h_f}, M_{A/H^\pm})$ [GeV]	$n_\gamma = 3$	$n_\gamma = 4$	$n_\gamma = 3$	$n_\gamma = 4$
BP1	(30 GeV, 355.5)	13.3%	7.2%	13.1%	7.2%
BP2	(30 GeV, 164.0)	30.7%	15.1%	31.3%	14.3%
BP3	(96 GeV, 428.3)	31.1%	39.9%	31.6%	40.1%
BP4	(96 GeV, 150.1)	36.3%	27.3%	36.6%	27.9%

TABLE II: Selection efficiencies for four benchmark points for the $4\gamma + W^+W^-$ and $4\gamma + W^\pm Z$ final states, including the off-shell V . Here n_γ is the number of photons that pass the cuts. The cuts are $p_T^\gamma > 10$ GeV, $|\eta^\gamma| < 2.5$, and $\Delta R(\gamma_i, \gamma_j) > 0.4$ at the detector level.

A critical question is whether we can discover the fermiophobic h_f via the multi-photon signals at the HL-LHC. We find that the SM backgrounds are almost negligible. Let us consider the process of $4\gamma + W^\pm$ as an example. The irreducible background, demanding four photons and one lepton with $p_T^\gamma > 10$ GeV, $p_T^\ell > 20$ GeV, $|\eta^{\gamma,\ell}| < 2.5$, and the isolation cuts of $\Delta R > 0.4$ where $\Delta R = \sqrt{(\Delta\eta)^2 + (\Delta\phi)^2}$ has the cross section about 1 ab [48]. If we require two gauge bosons associated with four photons, the irreducible backgrounds are totally negligible. The reducible backgrounds are from QCD jets accompanying one or two gauge bosons, with the QCD jet misidentified as a photon. But the mistagging probability is very small as $P_{j \rightarrow \gamma} \simeq 10^{-3}$ [102]. The final states with four photons require the multiplication of $P_{j \rightarrow \gamma}$ four times, which makes the reducible backgrounds also ignorable. Therefore, we conclude that the $4\gamma + VV'$ states have an almost background-free environment.

The final question is about the selection efficiencies of $4\gamma + VV'$. No matter how negligible the backgrounds are, small cross sections raise concerns about whether we can observe enough signal events especially when the selection efficiencies are very small. Full state-of-the-art simulations, customized for $4\gamma + W^+W^-$ and $4\gamma + W^\pm Z$, are beyond the scope of this letter. Here we present the detector-level selection efficiency only for four photons. Through a fast detector simulation of the signal using the DELPHES version 3.4.2 [103], we calculate $\epsilon_d = \sigma(\text{cuts})/\sigma(\text{no cuts})$. We demand $p_T^\gamma > 10$ GeV [48], $|\eta^\gamma| < 2.5$, and $\Delta R(\gamma_i, \gamma_j) > 0.4$. We take the following four benchmark points:

$$\begin{aligned}
\text{BP1: } & m_{h_f} = 30 \text{ GeV}, \quad M_{A/H^\pm} = 355.5 \text{ GeV}, \quad t_\beta = 13.6, \quad m_{12}^2 = 1.07 \text{ GeV}^2, \quad (15) \\
\text{BP2: } & m_{h_f} = 30 \text{ GeV}, \quad M_{A/H^\pm} = 164.0 \text{ GeV}, \quad t_\beta = 14.6, \quad m_{12}^2 = 0.97 \text{ GeV}^2, \\
\text{BP3: } & m_{h_f} = 96 \text{ GeV}, \quad M_{A/H^\pm} = 428.3 \text{ GeV}, \quad t_\beta = 4.8, \quad m_{12}^2 = 1663.0 \text{ GeV}^2, \\
\text{BP4: } & m_{h_f} = 96 \text{ GeV}, \quad M_{A/H^\pm} = 150.1 \text{ GeV}, \quad t_\beta = 26.6, \quad m_{12}^2 = 344.7 \text{ GeV}^2,
\end{aligned}$$

where BP1 and BP3 yield small signal rate of $4\gamma + VV'$ for $m_{h_f} = 30$ GeV and $m_{h_f} = 96$ GeV respectively while BP2 and BP4 yield large signal rate.

Table II shows the selection efficiency ϵ_d for the $4\gamma + W^+W^-$ and $4\gamma + ZW^\pm$ final states, focusing on four benchmark points in Eq. (15). Here we include the off-shell W and Z bosons. Since some photons decayed from the light h_f can fail to pass the cuts at the detector level, we separately present the selection efficiencies for $n_\gamma = 3$ and $n_\gamma = 4$, where n_γ is the number of photons that pass the cuts. In the case of $m_{h_f} = 30$ GeV, the selection efficiency with $n_\gamma = 3$ is larger than that with $n_\gamma = 4$. The light m_{h_f} tends to yield soft photons so that it is more probable for one of four photons to escape the detection. This tendency is stronger for BP2 where the smaller mass difference between m_{h_f} and M_{A/H^\pm} generates softer photons. If we relax the photon identification into $n_\gamma \geq 3$, therefore, the selection efficiency significantly increases: even the benchmark BP1 has the selection rate of about 20%, which can have a few thousand events with the total integrated luminosity of 3 ab^{-1} . In the case of $m_{h_f} = 96$ GeV, the efficiency for selecting four photons is significantly enhanced, about 40% for BP3 and about 27% for BP4. The mass of h_f is heavy enough to produce a pair of hard photons. If we include the events with $n_\gamma \geq 3$, the selection efficiency for $m_{h_f} = 96$ GeV is more than 70% for BP3 and 60% for BP4. Then even BP3 with the signal rate of $\mathcal{O}(0.1)$ fb can yield a few hundred events with the expected luminosity of 3 ab^{-1} . Considering almost background-free environment of $4\gamma + VV'$, we expect that the HL-LHC can probe the fermiophobic type-I.

V. CONCLUSIONS

The null results in the BSM searches at the LHC can coexist with an intermediate-mass new particle if the new particle is fermiophobic. Type-I in the 2HDM with the condition of $\alpha = \pi/2$ provides a fermiophobic Higgs boson, a lighter CP -even Higgs boson. The heavier CP -even Higgs boson describes the observed SM-like Higgs boson at a mass of 125 GeV. In this letter, we have studied the validity of the fermiophobic type-I not only at the electroweak scale but also at higher energy scale.

For the comprehensive study, we have first obtained the still-valid parameter space satisfying the theoretical requirements (bounded-from-below scalar potential, unitarity, perturbativity, vacuum stability), flavor-changing neutral currents in B physics, the cutoff scale above 1 TeV, Higgs precision data, and direct collider search bounds from the LEP, Tevatron, and LHC. For every viable parameter point, the cutoff scale Λ_c has been calculated through the RGE analysis. The most important result is that the fermiophobic type-I can maintain the theoretical validity all the way up to the Planck scale when the mass of the fermiophobic Higgs boson is larger than about 62.5 GeV. Even the mild condition of $\Lambda_c > 1$ TeV severely restricts the parameter space, which predicts definite signal rates of the BSM Higgs bosons in the multi-photon states at the LHC. Based on the studies of the decay rates and the production cross sections of the BSM Higgs bosons, we have suggested the $4\gamma + VV'$ processes as the golden discovery channels for the model since they enjoy almost background-free environment and substantial selection efficiencies.

Acknowledgments

The work of JK, SL, and JS is supported by the National Research Foundation of Korea, Grant No. NRF-2022R1A2C1007583. The work of P.S. was supported by the appointment to the JRG Program at the APCTP through the Science and Technology Promotion Fund and Lottery Fund of the Korean Government. This was also supported by the Korean Local Governments - Gyeongsangbuk-do Province and Pohang City.

-
- [1] A. G. Akeroyd, *Fermiophobic Higgs bosons at the Tevatron*, *Phys. Lett. B* **368** (1996) 89–95, [[hep-ph/9511347](#)].
 - [2] A. G. Akeroyd, *Fermiophobic and other nonminimal neutral Higgs bosons at the LHC*, *J. Phys. G* **24** (1998) 1983–1994, [[hep-ph/9803324](#)].
 - [3] A. G. Akeroyd, *Three body decays of Higgs bosons at LEP-2 and application to a hidden fermiophobic Higgs*, *Nucl. Phys. B* **544** (1999) 557–575, [[hep-ph/9806337](#)].
 - [4] A. Barroso, L. Brucher and R. Santos, *Is there a light fermiophobic Higgs?*, *Phys. Rev. D* **60** (1999) 035005, [[hep-ph/9901293](#)].
 - [5] L. Brucher and R. Santos, *Experimental signatures of fermiophobic Higgs bosons*, *Eur. Phys. J. C* **12** (2000) 87–98, [[hep-ph/9907434](#)].
 - [6] A. G. Akeroyd and M. A. Diaz, *Searching for a light fermiophobic Higgs boson at the Tevatron*, *Phys. Rev. D* **67** (2003) 095007, [[hep-ph/0301203](#)].
 - [7] A. G. Akeroyd, M. A. Diaz and F. J. Pacheco, *Double fermiophobic Higgs boson production at the CERN LHC and LC*, *Phys. Rev. D* **70** (2004) 075002, [[hep-ph/0312231](#)].
 - [8] A. G. Akeroyd, M. A. Diaz and M. A. Rivera, *Effect of Charged Scalar Loops on Photonic Decays of a Fermiophobic Higgs*, *Phys. Rev. D* **76** (2007) 115012, [[0708.1939](#)].
 - [9] A. Arhrib, R. Benbrik, R. B. Guedes and R. Santos, *Search for a light fermiophobic Higgs boson produced via gluon fusion at Hadron Colliders*, *Phys. Rev. D* **78** (2008) 075002, [[0805.1603](#)].
 - [10] E. Gabrielli, B. Mele and M. Raidal, *Has a fermiophobic Higgs boson been detected at the LHC?*, *Phys. Lett. B* **716** (2012) 322–325, [[1202.1796](#)].
 - [11] E. L. Berger, Z. Sullivan and H. Zhang, *Associated Higgs plus vector boson test of a fermiophobic Higgs boson*, *Phys. Rev. D* **86** (2012) 015011, [[1203.6645](#)].
 - [12] E. Gabrielli, K. Kannike, B. Mele, A. Racioppi and M. Raidal, *Fermiophobic Higgs Boson and Supersymmetry*, *Phys. Rev. D* **86** (2012) 055014, [[1204.0080](#)].
 - [13] H. Cardenas, A. C. B. Machado, V. Pleitez and J. A. Rodriguez, *Higgs decay rate to two photons in a model with two fermiophobic-Higgs doublets*, *Phys. Rev. D* **87** (2013) 035028, [[1212.1665](#)].
 - [14] V. Ilisie and A. Pich, *Low-mass fermiophobic charged Higgs phenomenology in two-Higgs-doublet models*, *JHEP* **09** (2014) 089, [[1405.6639](#)].
 - [15] A. Delgado, M. Garcia-Pepin, M. Quiros, J. Santiago and R. Vega-Morales, *Diphoton and*

- Diboson Probes of Fermiophobic Higgs Bosons at the LHC*, *JHEP* **06** (2016) 042, [[1603.00962](#)].
- [16] T. Mondal and P. Sanyal, *Same sign trilepton as signature of charged Higgs in two Higgs doublet model*, *JHEP* **05** (2022) 040, [[2109.05682](#)].
- [17] A. Donini, F. Feruglio, J. Matias and F. Zwirner, *Phenomenological aspects of a fermiophobic $SU(2) \times SU(2) \times U(1)$ extension of the standard model*, *Nucl. Phys. B* **507** (1997) 51–90, [[hep-ph/9705450](#)].
- [18] T. Ohl and C. Speckner, *Production of Almost Fermiophobic Gauge Bosons in the Minimal Higgsless Model at the LHC*, *Phys. Rev. D* **78** (2008) 095008, [[0809.0023](#)].
- [19] J. Bramante, R. S. Hundi, J. Kumar, A. Rajaraman and D. Yaylali, *Collider Searches for Fermiophobic Gauge Bosons*, *Phys. Rev. D* **84** (2011) 115018, [[1106.3819](#)].
- [20] F. Bach and T. Ohl, *Discovery Prospects of an Almost Fermiophobic W' in the Three-Site Higgsless Model at the LHC*, *Phys. Rev. D* **85** (2012) 015002, [[1111.1551](#)].
- [21] N. Chen, Y. Zhang, Q. Wang, G. Cacciapaglia, A. Deandrea and L. Panizzi, *Higgsphobic and fermiophobic Z' as a single dark matter candidate*, *JHEP* **05** (2014) 088, [[1403.2918](#)].
- [22] B. Coleppa, S. Kumar and A. Sarkar, *Fermiophobic gauge boson phenomenology in 221 Models*, *Phys. Rev. D* **98** (2018) 095009, [[1808.09728](#)].
- [23] M. F. Navarro and S. F. King, *Fermiophobic Z' model for simultaneously explaining the muon anomalies $RK^{(*)}$ and $(g-2)_\mu$* , *Phys. Rev. D* **105** (2022) 035015, [[2109.08729](#)].
- [24] B. Fu and S. F. King, *Spontaneously stabilised dark matter from a fermiophobic $U(1)$ ' gauge symmetry*, *JHEP* **12** (2021) 121, [[2110.00588](#)].
- [25] A. M. Thalapillil, *Bound states and fermiophobic Unparticle oblique corrections to the photon*, *Phys. Rev. D* **81** (2010) 035001, [[0906.4379](#)].
- [26] DELPHI collaboration, P. Abreu et al., *Search for a fermiophobic Higgs at LEP-2*, *Phys. Lett. B* **507** (2001) 89–103, [[hep-ex/0104025](#)].
- [27] DELPHI collaboration, J. Abdallah et al., *Search for fermiophobic Higgs bosons in final states with photons at LEP 2*, *Eur. Phys. J. C* **35** (2004) 313–324, [[hep-ex/0406012](#)].
- [28] D0 collaboration, V. M. Abazov et al., *Search for decay of a fermiophobic Higgs boson $h(f) \rightarrow \gamma\gamma$ with the D0 detector at $\sqrt{s} = 1.96\text{-TeV}$* , *Phys. Rev. Lett.* **101** (2008) 051801, [[0803.1514](#)].
- [29] CDF collaboration, T. Aaltonen et al., *Search for a Fermiophobic Higgs Boson Decaying into Diphotons in p anti- p Collisions at $s^{**}(1/2) = 1.96\text{-TeV}$* , *Phys. Rev. Lett.* **103** (2009) 061803, [[0905.0413](#)].
- [30] D0 collaboration, V. M. Abazov et al., *Search for the standard model and a fermiophobic Higgs boson in diphoton final states*, *Phys. Rev. Lett.* **107** (2011) 151801, [[1107.4587](#)].
- [31] CDF, D0, TEVATRON NEW HIGGS WORKING GROUP collaboration, *Combined CDF and D0 Upper Limits on Fermiophobic Higgs Boson Production with up to 8.2 fb^{-1} of $p\bar{p}$ data*, in *19th International Conference on Supersymmetry and Unification of Fundamental Interactions*, 9, 2011. [[1109.0576](#)].

- [32] CMS collaboration, *Search for the fermiophobic model Higgs boson decaying into two photons*, .
- [33] ATLAS collaboration, G. Aad et al., *Search for a fermiophobic Higgs boson in the diphoton decay channel with the ATLAS detector*, *Eur. Phys. J. C* **72** (2012) 2157, [1205.0701].
- [34] CMS collaboration, S. Chatrchyan et al., *Search for a Fermiophobic Higgs Boson in pp Collisions at $\sqrt{s} = 7$ TeV*, *JHEP* **09** (2012) 111, [1207.1130].
- [35] CMS collaboration, S. Chatrchyan et al., *Searches for Higgs Bosons in pp Collisions at $\sqrt{s} = 7$ and 8 TeV in the Context of Four-Generation and Fermiophobic Models*, *Phys. Lett. B* **725** (2013) 36–59, [1302.1764].
- [36] ATLAS collaboration, G. Aad et al., *Combined measurements of Higgs boson production and decay using up to 80 fb⁻¹ of proton-proton collision data at $\sqrt{s} = 13$ TeV collected with the ATLAS experiment*, *Phys. Rev. D* **101** (2020) 012002, [1909.02845].
- [37] CMS collaboration, A. M. Sirunyan et al., *Evidence for Higgs boson decay to a pair of muons*, *JHEP* **01** (2021) 148, [2009.04363].
- [38] ATLAS collaboration, *Combined measurements of Higgs boson production and decay using up to 139 fb⁻¹ of proton-proton collision data at $\sqrt{s} = 13$ TeV collected with the ATLAS experiment*, .
- [39] J. Bernon, J. F. Gunion, H. E. Haber, Y. Jiang and S. Kraml, *Scrutinizing the alignment limit in two-Higgs-doublet models. II. $m_H = 125$ GeV*, *Phys. Rev. D* **93** (2016) 035027, [1511.03682].
- [40] S. Chang, S. K. Kang, J.-P. Lee and J. Song, *Higgs potential and hidden light Higgs scenario in two Higgs doublet models*, *Phys. Rev. D* **92** (2015) 075023, [1507.03618].
- [41] A. Jueid, J. Kim, S. Lee and J. Song, *Type-X two-Higgs-doublet model in light of the muon $g-2$: Confronting Higgs boson and collider data*, *Phys. Rev. D* **104** (2021) 095008, [2104.10175].
- [42] S. Lee, K. Cheung, J. Kim, C.-T. Lu and J. Song, *Status of the two-Higgs-doublet model in light of the CDF m_W measurement*, 2204.10338.
- [43] P. Bechtle, S. Heinemeyer, T. Klingl, T. Stefaniak, G. Weiglein and J. Wittbrodt, *HiggsSignals-2: Probing new physics with precision Higgs measurements in the LHC 13 TeV era*, *Eur. Phys. J. C* **81** (2021) 145, [2012.09197].
- [44] P. Bechtle, D. Dercks, S. Heinemeyer, T. Klingl, T. Stefaniak, G. Weiglein et al., *HiggsBounds-5: Testing Higgs Sectors in the LHC 13 TeV Era*, *Eur. Phys. J. C* **80** (2020) 1211, [2006.06007].
- [45] CDF collaboration, T. A. Aaltonen et al., *Search for a Low-Mass Neutral Higgs Boson with Suppressed Couplings to Fermions Using Events with Multiphoton Final States*, *Phys. Rev. D* **93** (2016) 112010, [1601.00401].
- [46] CMS collaboration, *Search for exotic decay of the Higgs boson into two light pseudoscalars with four photons in the final state at $\sqrt{s} = 13$ TeV*, .
- [47] A. G. Akeroyd, A. Alves, M. A. Diaz and O. J. P. Eboli, *Multi-photon signatures at the Fermilab Tevatron*, *Eur. Phys. J. C* **48** (2006) 147–157, [hep-ph/0512077].
- [48] A. Arhrib, R. Benbrik, R. Enberg, W. Klemm, S. Moretti and S. Munir, *Identifying a light charged Higgs boson at the LHC Run II*, *Phys. Lett. B* **774** (2017) 591–598, [1706.01964].

- [49] G. C. Branco, P. M. Ferreira, L. Lavoura, M. N. Rebelo, M. Sher and J. P. Silva, *Theory and phenomenology of two-Higgs-doublet models*, *Phys. Rept.* **516** (2012) 1–102, [[1106.0034](#)].
- [50] S. L. Glashow and S. Weinberg, *Natural Conservation Laws for Neutral Currents*, *Phys. Rev. D* **15** (1977) 1958.
- [51] E. A. Paschos, *Diagonal Neutral Currents*, *Phys. Rev. D* **15** (1977) 1966.
- [52] J. Song and Y. W. Yoon, *$W\gamma$ decay of the elusive charged Higgs boson in the two-Higgs-doublet model with vectorlike fermions*, *Phys. Rev. D* **100** (2019) 055006, [[1904.06521](#)].
- [53] D. Eriksson, J. Rathsmann and O. Stal, *2HDMC: Two-Higgs-Doublet Model Calculator Physics and Manual*, *Comput. Phys. Commun.* **181** (2010) 189–205, [[0902.0851](#)].
- [54] I. P. Ivanov, *Minkowski space structure of the Higgs potential in 2HDM*, *Phys. Rev. D* **75** (2007) 035001, [[hep-ph/0609018](#)].
- [55] A. Arhrib, *Unitarity constraints on scalar parameters of the standard and two Higgs doublets model*, in *Workshop on Noncommutative Geometry, Superstrings and Particle Physics*, 12, 2000. [hep-ph/0012353](#).
- [56] I. P. Ivanov, *General two-order-parameter Ginzburg-Landau model with quadratic and quartic interactions*, *Phys. Rev. E* **79** (2009) 021116, [[0802.2107](#)].
- [57] A. Barroso, P. M. Ferreira, I. P. Ivanov, R. Santos and J. P. Silva, *Evading death by vacuum*, *Eur. Phys. J. C* **73** (2013) 2537, [[1211.6119](#)].
- [58] A. Barroso, P. M. Ferreira, I. P. Ivanov and R. Santos, *Metastability bounds on the two Higgs doublet model*, *JHEP* **06** (2013) 045, [[1303.5098](#)].
- [59] M. E. Peskin and T. Takeuchi, *Estimation of oblique electroweak corrections*, *Phys. Rev. D* **46** (1992) 381–409.
- [60] PARTICLE DATA GROUP collaboration, P. A. Zyla et al., *Review of Particle Physics*, *PTEP* **2020** (2020) 083C01.
- [61] H.-J. He, N. Polonsky and S.-f. Su, *Extra families, Higgs spectrum and oblique corrections*, *Phys. Rev. D* **64** (2001) 053004, [[hep-ph/0102144](#)].
- [62] W. Grimus, L. Lavoura, O. M. Ogreid and P. Osland, *The Oblique parameters in multi-Higgs-doublet models*, *Nucl. Phys. B* **801** (2008) 81–96, [[0802.4353](#)].
- [63] A. Arbey, F. Mahmoudi, O. Stal and T. Stefaniak, *Status of the Charged Higgs Boson in Two Higgs Doublet Models*, *Eur. Phys. J. C* **78** (2018) 182, [[1706.07414](#)].
- [64] M. Misiak and M. Steinhauser, *Weak radiative decays of the B meson and bounds on M_{H^\pm} in the Two-Higgs-Doublet Model*, *Eur. Phys. J. C* **77** (2017) 201, [[1702.04571](#)].
- [65] J. Oredsson and J. Rathsmann, *Z_2 breaking effects in 2-loop RG evolution of 2HDM*, *JHEP* **02** (2019) 152, [[1810.02588](#)].
- [66] J. Oredsson, *2HDME : Two-Higgs-Doublet Model Evolver*, *Comput. Phys. Commun.* **244** (2019) 409–426, [[1811.08215](#)].
- [67] ATLAS collaboration, M. Aaboud et al., *Search for Higgs bosons produced via vector-boson fusion and decaying into bottom quark pairs in $\sqrt{s} = 13$ TeV pp collisions with the ATLAS detector*, *Phys. Rev. D* **98** (2018) 052003, [[1807.08639](#)].

- [68] ATLAS collaboration, M. Aaboud et al., *Measurements of gluon-gluon fusion and vector-boson fusion Higgs boson production cross-sections in the $H \rightarrow WW^* \rightarrow e\nu\mu\nu$ decay channel in pp collisions at $\sqrt{s} = 13$ TeV with the ATLAS detector*, *Phys. Lett. B* **789** (2019) 508–529, [[1808.09054](#)].
- [69] ATLAS collaboration, M. Aaboud et al., *Cross-section measurements of the Higgs boson decaying into a pair of τ -leptons in proton-proton collisions at $\sqrt{s} = 13$ TeV with the ATLAS detector*, *Phys. Rev. D* **99** (2019) 072001, [[1811.08856](#)].
- [70] ATLAS collaboration, G. Aad et al., *Higgs boson production cross-section measurements and their EFT interpretation in the 4ℓ decay channel at $\sqrt{s} = 13$ TeV with the ATLAS detector*, *Eur. Phys. J. C* **80** (2020) 957, [[2004.03447](#)].
- [71] CMS collaboration, A. M. Sirunyan et al., *Search for $t\bar{t}H$ production in the $H \rightarrow b\bar{b}$ decay channel with leptonic $t\bar{t}$ decays in proton-proton collisions at $\sqrt{s} = 13$ TeV*, *JHEP* **03** (2019) 026, [[1804.03682](#)].
- [72] CMS collaboration, A. M. Sirunyan et al., *Search for the Higgs boson decaying to two muons in proton-proton collisions at $\sqrt{s} = 13$ TeV*, *Phys. Rev. Lett.* **122** (2019) 021801, [[1807.06325](#)].
- [73] CMS collaboration, *Measurements of properties of the Higgs boson in the four-lepton final state in proton-proton collisions at $\sqrt{s} = 13$ TeV*, .
- [74] CMS collaboration, *Measurements of differential Higgs boson production cross sections in the leptonic WW decay mode at $\sqrt{s} = 13$ TeV*, .
- [75] ATLAS collaboration, G. Aad et al., *Search for new phenomena in events with at least three photons collected in pp collisions at $\sqrt{s} = 8$ TeV with the ATLAS detector*, *Eur. Phys. J. C* **76** (2016) 210, [[1509.05051](#)].
- [76] LEP collaboration, A. Rosca, *Fermiophobic Higgs bosons at LEP*, *Nucl. Phys. B Proc. Suppl.* **117** (2003) 743, [[hep-ex/0212038](#)].
- [77] ATLAS collaboration, M. Aaboud et al., *Search for charged Higgs bosons decaying via $H^\pm \rightarrow \tau^\pm\nu_\tau$ in the τ +jets and τ +lepton final states with 36 fb^{-1} of pp collision data recorded at $\sqrt{s} = 13$ TeV with the ATLAS experiment*, *JHEP* **09** (2018) 139, [[1807.07915](#)].
- [78] ATLAS collaboration, *Search for resonances in the 65 to 110 GeV diphoton invariant mass range using 80 fb^{-1} of pp collisions collected at $\sqrt{s} = 13$ TeV with the ATLAS detector*, .
- [79] ATLAS collaboration, *Search for heavy resonances decaying into a Z boson and a Higgs boson in final states with leptons and b-jets in 139 fb^{-1} of pp collisions at $\sqrt{s} = 13\text{TeV}$ with the ATLAS detector*, .
- [80] CDF collaboration, T. Aaltonen et al., *High-precision measurement of the W boson mass with the CDF II detector*, *Science* **376** (2022) 170–176.
- [81] C.-T. Lu, L. Wu, Y. Wu and B. Zhu, *Electroweak Precision Fit and New Physics in light of W Boson Mass*, [2204.03796](#).
- [82] Y.-Z. Fan, T.-P. Tang, Y.-L. S. Tsai and L. Wu, *Inert Higgs Dark Matter for New CDF W-boson Mass and Detection Prospects*, [2204.03693](#).
- [83] C.-R. Zhu, M.-Y. Cui, Z.-Q. Xia, Z.-H. Yu, X. Huang, Q. Yuan et al., *GeV*

- antiproton/gamma-ray excesses and the W -boson mass anomaly: three faces of $\sim 60 - 70$ GeV dark matter particle?*, [2204.03767](#).
- [84] B.-Y. Zhu, S. Li, J.-G. Cheng, R.-L. Li and Y.-F. Liang, *Using gamma-ray observation of dwarf spheroidal galaxy to test a dark matter model that can interpret the W -boson mass anomaly*, [2204.04688](#).
- [85] H. Song, W. Su and M. Zhang, *Electroweak Phase Transition in 2HDM under Higgs, Z-pole, and W precision measurements*, [2204.05085](#).
- [86] H. Bahl, J. Braathen and G. Weiglein, *New physics effects on the W -boson mass from a doublet extension of the SM Higgs sector*, [2204.05269](#).
- [87] Y. Heo, D.-W. Jung and J. S. Lee, *Impact of the CDF W -mass anomaly on two Higgs doublet model*, [2204.05728](#).
- [88] K. S. Babu, S. Jana and V. P. K., *Correlating W -Boson Mass Shift with Muon $g - 2$ in the 2HDM*, [2204.05303](#).
- [89] T. Biekötter, S. Heinemeyer and G. Weiglein, *Excesses in the low-mass Higgs-boson search and the W -boson mass measurement*, [2204.05975](#).
- [90] Y. H. Ahn, S. K. Kang and R. Ramos, *Implications of New CDF-II W Boson Mass on Two Higgs Doublet Model*, [2204.06485](#).
- [91] X.-F. Han, F. Wang, L. Wang, J. M. Yang and Y. Zhang, *A joint explanation of W -mass and muon $g-2$ in 2HDM*, [2204.06505](#).
- [92] G. Arcadi and A. Djouadi, *The 2HD+a model for a combined explanation of the possible excesses in the CDF M_W measurement and $(g - 2)_\mu$ with Dark Matter*, [2204.08406](#).
- [93] K. Ghorbani and P. Ghorbani, *W -Boson Mass Anomaly from Scale Invariant 2HDM*, [2204.09001](#).
- [94] A. Broggio, E. J. Chun, M. Passera, K. M. Patel and S. K. Vempati, *Limiting two-Higgs-doublet models*, *JHEP* **11** (2014) 058, [[1409.3199](#)].
- [95] J. Kim, S. Lee, P. Sanyal and J. Song, *CDF W boson mass and muon $g - 2$ in type- X two-Higgs-doublet model with a Higgs-phobic light pseudoscalar*, [2205.01701](#).
- [96] K. Cheung, A. Jueid, J. Kim, S. Lee, C.-T. Lu and J. Song, *Comprehensive study of the light charged Higgs boson in the type-I two-Higgs-doublet model*, *Phys. Rev. D* **105** (2022) 095044, [[2201.06890](#)].
- [97] S. Banerjee, B. Bhattacharjee, A. Goudelis, B. Herrmann, D. Sengupta and R. Sengupta, *Determining the lifetime of long-lived particles at the HL-LHC*, *Eur. Phys. J. C* **81** (2021) 172, [[1912.06669](#)].
- [98] A. Alloul, N. D. Christensen, C. Degrande, C. Duhr and B. Fuks, *FeynRules 2.0 - A complete toolbox for tree-level phenomenology*, *Comput. Phys. Commun.* **185** (2014) 2250–2300, [[1310.1921](#)].
- [99] C. Degrande, C. Duhr, B. Fuks, D. Grellscheid, O. Mattelaer and T. Reiter, *UFO - The Universal FeynRules Output*, *Comput. Phys. Commun.* **183** (2012) 1201–1214, [[1108.2040](#)].
- [100] J. Alwall, M. Herquet, F. Maltoni, O. Mattelaer and T. Stelzer, *MadGraph 5 : Going Beyond*,

- JHEP* **06** (2011) 128, [[1106.0522](#)].
- [101] NNPDF collaboration, R. D. Ball et al., *Parton distributions from high-precision collider data*, *Eur. Phys. J. C* **77** (2017) 663, [[1706.00428](#)].
- [102] Y. Wang, A. Arhrib, R. Benbrik, M. Krab, B. Manaut, S. Moretti et al., *Analysis of $W^\pm + 4\gamma$ in the 2HDM Type-I at the LHC*, *JHEP* **12** (2021) 021, [[2107.01451](#)].
- [103] DELPHES 3 collaboration, J. de Favereau, C. Delaere, P. Demin, A. Giammanco, V. Lemaitre, A. Mertens et al., *DELPHES 3, A modular framework for fast simulation of a generic collider experiment*, *JHEP* **02** (2014) 057, [[1307.6346](#)].